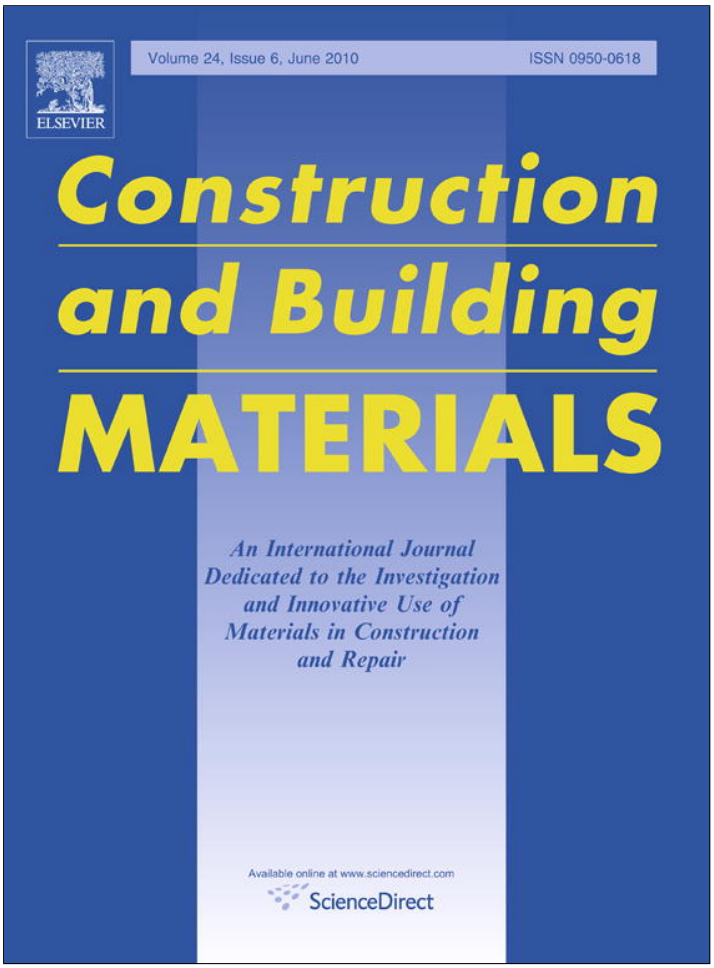

Construction and Building Materials 24 (2010) 1078–1085

Contents lists available at ScienceDirect

Construction and Building Materials

journal homepage: www.elsevier.com/locate/conbuildmat

Placing conditions, mesostructural characteristics and post-cracking response of fibre reinforced self-compacting concretes

María C. Torrijos [a,*], Bryan E. Barragán [b], Raúl L. Zerbino [a]

[a] CONICET, Faculty of Engineering UNLP, LEMIT-CIC, La Plata, Argentina
[b] BASF Construction Chemicals, Admixture Systems Europe, Treviso, Italy

ARTICLE INFO

Article history:
Received 10 June 2009
Received in revised form 17 November 2009
Accepted 18 November 2009
Available online 16 December 2009

Keywords:
Fibre reinforced self-compacting concrete
Placing conditions
Fibre density
Fibre distribution
Fibre orientation
Post-peak flexural behaviour

ABSTRACT

The benefits of adding fibres to concrete, evidenced in the post-cracking behaviour, are strongly influenced not only by the type and content of fibres but also by their orientation. The objective of this study is to evaluate the influence of the casting/placing procedure on the post-peak behaviour of fibre reinforced self-compacting concrete, and its relationship with the mesostructural characteristics of the material (type, distribution and orientation of fibres). Three concretes were prepared using two types of steel fibres of different lengths (50 mm and 30 mm) and a structural type polymer fibre. Beams of 150 × 150 × 600 mm were cast in three different ways: filling the moulds from the centre in accordance with the EN 14651 Standard, pouring concrete from one end of the mould after a flowing along a 5 m length and 150 mm diameter pipe, and finally, filling the moulds vertically. Flexural tests according to the European Standard indicate that the three types of fibres achieve a preferential orientation along horizontal planes, like in conventional vibrated fibre reinforced concrete. The mechanical response of beams cast with longer steel fibres was strongly affected by the casting procedure while the flexural performance of the other two fibre concretes, was less affected. Such results are well in accordance with the density of fibres measured by fibre counting in different cut planes.

1. Introduction

The benefits of adding fibres to concrete, improving ductility through crack control, and providing residual load-bearing capacity, have been widely informed along the past four decades. The post-peak behaviour is influenced by the type, content and orientation of fibres [1,2]. Several studies have demonstrated that there is a high level of proportionality between the fibres counted in the fracture surface and the toughness [1,3]. Kooiman [1] observed that the variability in the post-peak parameters measured through the bending test were related to the fibre distribution in the cross section. In other studies on fibre reinforced concrete (FRC) [4–6] it was also observed that the variability on the results from the uniaxial tension test can be justified considering the effect of the number of fibres in the crack sections.

The fibre distribution is an important aspect to be considered for the design and the analysis of the structural response of fibre concrete elements. Although the distribution of fibres could be homogeneous after the mixing process, the casting and compaction processes, together with wall effects, affect fibre orientation [1,7,8]. Many authors agree that in conventionally vibrated FRC fibres acquire a 2D orientation in horizontal planes [1,9–12]. Recent studies have investigated the distribution of steel fibres in fibre reinforced self-compacting concrete (FR-SCC), showing that fibre orientation is related to the flow characteristics of the FR-SCC [15], that fibres are prone to be aligned in the flow direction [7,13,14], and that this effect increases with the flowability of the FR-SCC [8]. Regarding the influence of the fibre type, a recent study [14] indicates that the influence of the fibre length on the fibre alignment is negligible. Others show that, especially for fibres of high aspect ratio, the higher fine to coarse aggregate ratios enhanced the orientation of fibres beams for standard flexure tests [15].

This paper studies the influence of the casting procedure on the post-peak behaviour of FR-SCC incorporating steel fibres of different length and a structural polymer fibre, and its relationship with the mesostructural characteristics of the material (type, distribution and orientation of fibres).

2. Experimental program

2.1. Materials and mix design

Three FR-SCC were prepared from the same base mixture, with a water/cement ratio equal to 0.47. Component materials include CEM I 52.5 R, limestone filler, crushed limestone aggregates; combinations of 0–2 mm and 0–5 mm sands, and

* Corresponding author. Tel.: +54 2214831142; fax: +54 2214250471.
E-mail address: celestetorrijos@hotmail.com (M.C. Torrijos).

0950-0618/$ - see front matter © 2009 Elsevier Ltd. All rights reserved.
doi:10.1016/j.conbuildmat.2009.11.008

Table 1
Mix proportions and fresh concrete properties.

Concrete	FR-SCC1	FR-SCC2	FR-SCC3
Mix proportions (kg/m^3)			
Cement	343		343
Limestone filler	103		103
Water	161		170
Sand 0–2 mm	619		619
Sand 0–5 mm	346		346
Gravel 5–12 mm	462		462
Gravel 12–18 mm	337		337
Plasticizer	2.8		3.4
Superplasticizer	11.3		11.3
Type of fibre	F1 (steel)	F2 (steel)	F3 (polymeric)
	35	35	2.5
Fresh concrete properties			
Slump flow D_f (mm)	540	590	500
Slump flow t_{50} (s)	2.6	3.2	5.3
V-funnel T_V (s)	9.7	19.5	9.0
J-ring D_j (mm)	505	535	460

5–12 mm and 12–18 mm gravels. The mix proportions are given in Table 1. Steel fibres were of the hook-end type, FR-SCC1 incorporates 50 mm length and 1 mm diameter fibres, while FR-SCC2 incorporates 30 mm long and 0.38 mm diameter fibres. FR-SCC3 incorporates polymer fibres of 54 mm length. Admixtures include a poly-functional plasticizer and a polycarboxylate-based high-range water reducing admixture, Glenium C303 SCC superplasticizer.

Table 1 also shows the fresh concrete properties evaluated through the slump-flow (D_f and t_{50}), J-ring (D_j) and V-funnel (T_V), according to the Spanish Standards UNE 83361, UNE 83362, and UNE 83364, respectively. As it can be seen from Table 1, an increase of the V-funnel time, T_V, is observed in the case of FR-SCC2, which can be attributed to the higher slenderness of the FR-SCC2 fibres (aspect ratio = 80) compared to the FR-SCC1 fibres (aspect ratio = 50). Note that for the same fibre dosage (35 kg/m^3) the number of fibres in FR-SCC2 is much higher than in FR-SCC1.

2.2. Test specimens

Twelve beams of size 150 × 150 × 600 mm were cast with each FR-SCC, with the casting arrangements shown in Fig. 1; four beams were cast according to EN 14651 Standard, pouring the concrete from the centre of the mould (C). Other four beams were cast after the FR-SCC had flowed along a tube (T) of 5 m length, 150 mm diameter, and 20° slope, pouring the concrete from one end of the mould. Finally, four beams were cast with the moulds placed in a vertical position (V), and the concrete poured from the top. In the case of T beams, the halves including the end from where the concrete was poured were called A, and the opposite halves were called B. In V beams the top and the bottom halves were called A and B respectively. Then, in both cases concrete flowed from A to B.

All specimens were cured during 28 days in a moisture room (20 ± 2 °C, 98 ± 2% RH).

2.3. Flexure tests

Three point loading flexural tests on notched specimens were carried out in accordance with EN 14651 Standard, measuring the limit of proportionality (LOP) or first-peak strength in this case (f_L), and the residual strengths at 0.5, 1.5, 2.5, and 3.5 mm of crack mouth opening displacement (CMOD), f_{R1}, f_{R2}, f_{R3}, and f_{R4}, respectively. Also, the maximum flexural strength (f_M) along the entire post-peak regime was obtained. Tests were performed in a servo-hydraulic Instron testing system through crack width control, using a clip type extensometer, the test configuration can be observed in Fig. 2.

2.4. Fibre orientation and distribution

After the bending tests, the fibre orientation and distribution was studied by analysing the fibre density in three orthogonal planes of three beams cast with FR-SCC1 and FR-SCC2. In the case of FR-SCC3 beams, such measures were not obtained due to the high difficultly to precisely count the polymer fibres in the concrete matrix by visual observation.

The steel fibre density was analysed by cutting the beams halves (after the flexure tests) in three directions: transversally (α), longitudinal–perpendicular to the cast side (γ), and longitudinal–parallel to the cast side (β), as it is shown in Fig. 3. For the beams cast horizontally, a transversal cut on each half was performed first. Afterwards, one half of the tested beam was cut along the longitudinal–parallel direction, and the other half, in the longitudinal–perpendicular direction. Each half of the T and V beams was cut in the three directions.

The fibre distribution along planes α, β, and γ was also considered to evaluate the influence of the concrete flow along the moulds and expected wall effects. Each plane was divided in three or nine zones in accordance with the concrete flow and the number of fibres was counted in each zone, as it can be seen in Fig. 4.

The fibre density in all the cut sections was calculated by obtaining the mean number of fibres per unit area.

3. Results

3.1. Mechanical properties

Bending tests were performed at the age of 28 days. Fig. 5 shows the individual load–CMOD curves obtained for groups C, T and V of each concrete.

In FR-SCC1, T beams achieved the highest post-peak strength, with a post-peak hardening producing residual strengths quite above the first-peak stress. The C beams showed an intermediate performance, with less hardening after the first-peak drop and lower residual strengths than the T beams. On the contrary, V beams did not present any hardening along the post-peak regime, showing residual stresses of approximately 40% of the first-peak stress (LOP).

In FR-SCC2, which incorporates shorter steel fibres, the differences due to the casting arrangements were not as evident as in FR-SCC1. Both C and T beams showed a similar post-peak behav-

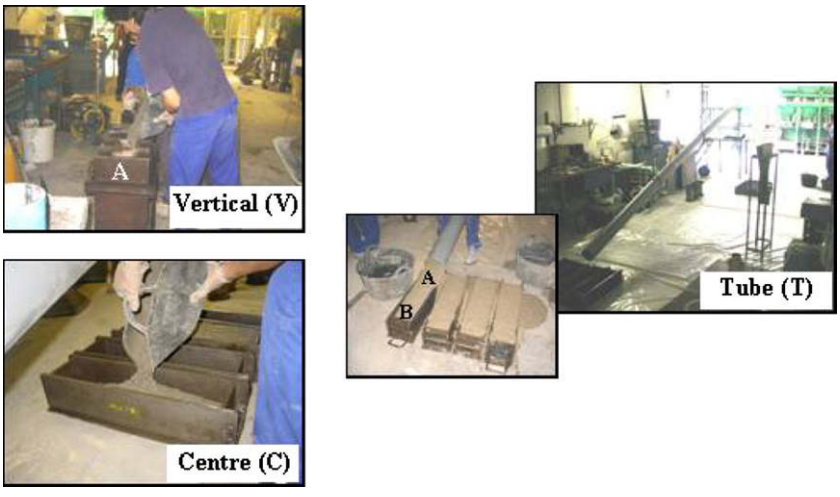

Fig. 1. Casting arrangements.

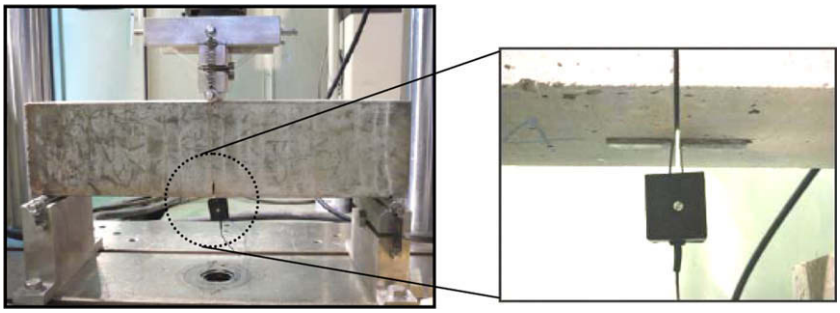

Fig. 2. Flexure test arrangement according to EN 14651 and detail of the device used to measure the CMOD.

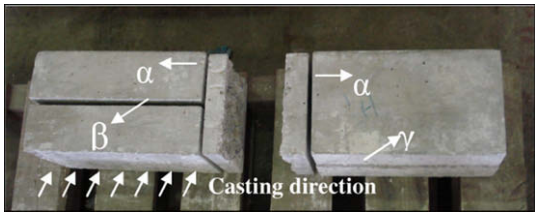

Fig. 3. Planes α, β and γ for the analysis of the fibre orientation.

iour (hardening type). In the case of T beams, the post-peak curves presented a small increase in variability, mainly at early stages, which is evidenced in the scatter of f_M and f_{R1} results. As happened in the case of FR-SCC1, V beams showed the lowest residual strength.

Finally, in FR-SCC3 incorporating polymer fibres, neither C, T nor V beams presented a hardening response in the post-peak stage. However, as it happened in the FR-SCC1 and FR-SCC2 concretes, the post-peak performance is clearly lower in the V beams (cast vertically). It can also be seen that C and T beams had a similar behaviour, as in FR-SCC2, indicating that the differences between the two casting arrangements were negligible.

The observed behaviour is confirmed by the analysis of the mean values of the residual strengths measured from the flexure tests (f_L, f_{R1}, f_{R2}, f_{R3}, f_{R4}, and f_M), summarised in Table 2.

With the aim of analysing the effect of the casting procedures on the mechanical behaviour of FR-SCC, results included in Table 2 are plotted as relative values in Fig. 6, considering C beams as the reference. It can be seen that in FR-SCC1 the residual strengths of T beams were between 163% and 175% of the strengths of C beams, while in FR-SCC2 and FR-SCC3 the values were between 75–97% and 92–100%, respectively. As it again can be seen, when compared to the SCC with longer steel fibres (FR-SCC1), concretes FR-SCC2 and FR-SCC3 show less differences between the case where the material flowed along the tube and the mould, and the case where the specimens were cast according to the standard indications, which present a slightly higher post-peak response. In the case of V beams, in FR-SCC1 the residual strengths were in the order of 36–38% of the residual strengths of C beams but FR-SCC2 beams showed values between 53% and 71%. In FR-SCC3 the strengths were between 27% and 33% of the residual strengths of C beams.

3.2. Fibres orientation and distribution

Table 3 presents the results of the fibre density measured in different directions for each group of beams of concretes FR-SCC1 and FR-SCC2; standard deviations are included between parentheses. Considering FR-SCC1, it can be seen that in the V beams the density of fibres was similar in planes β and γ (0.35 fibres/cm^2) and smaller in the transversal plane (0.23 fibres/

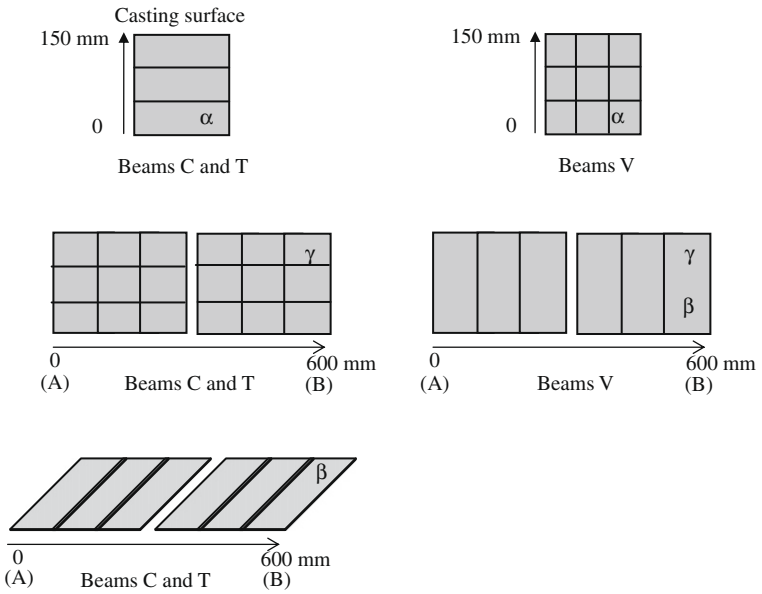

Fig. 4. Template for the analysis of the fibre distribution in the different planes of the beams.

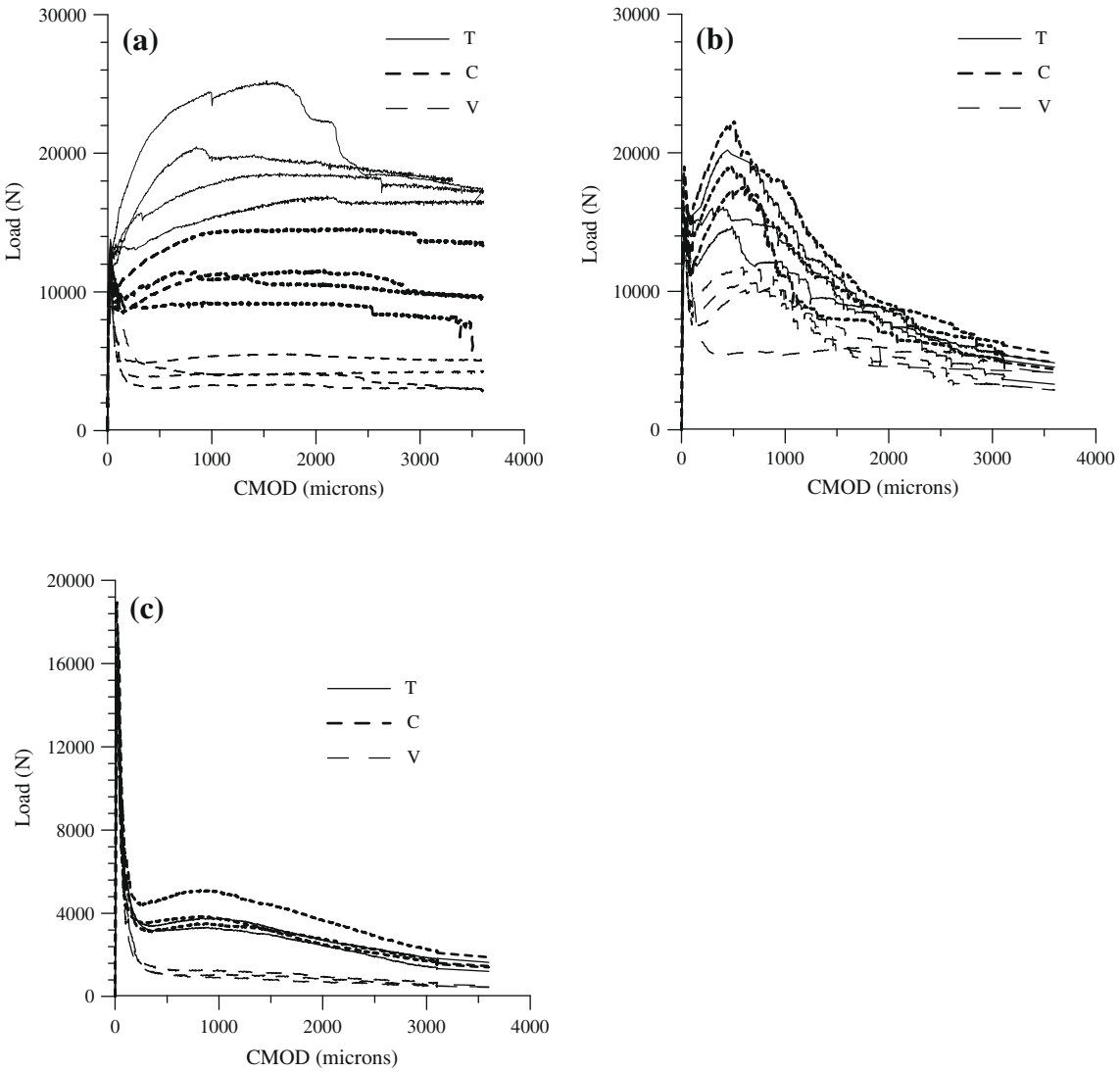

Fig. 5. Load–CMOD response from flexure tests: (a) FR-SCC1, (b) FR-SCC2, (c) FR-SCC3.

Table 2
Flexural test results with corresponding standard deviation.

Concrete	Beams	Residual strength parameters (MPa)					
		f_L	f_{R1}	f_{R2}	f_{R3}	f_{R4}	f_M
FR-SCC1	C	3.8 (0.3)	3.4 (0.5)	3.6 (0.7)	3.5 (0.7)	3.2 (0.8)	4.0 (0.5)
	T	4.2 (0.1)	5.6 (1.2)	6.3 (1.3)	5.7 (0.4)	5.5 (0.3)	6.4 (1.2)
	V	3.2 (0.25)	1.3 (0.3)	1.3 (0.3)	1.3 (0.3)	1.2 (0.3)	3.3 (0.2)
FR-SCC2	C	5.4 (0.3)	5.5 (1.0)	3.1 (0.7)	2.1 (0.3)	1.6 (0.3)	5.8 (0.6)
	T	4.4 (0.3)	4.9 (1.2)	3.0 (0.4)	1.8 (0.2)	1.2 (0.2)	5.1 (1.1)
	V	5.1 (0.1)	2.9 (0.8)	2.0 (0.2)	1.5 (0.2)	1.0 (0.2)	5.1 (0.1)
FR-SCC3	C	5.4 (0.6)	1.2 (0.2)	1.1 (0.2)	0.7 (0.1)	0.5 (0.1)	5.4 (0.6)
	T	5.2 (0.3)	1.1 (0.1)	1.0 (0.1)	0.7 (0.1)	0.5 (0.1)	5.2 (0.3)
	V	4.9 (0.4)	0.4 (0.04)	0.3 (0.05)	0.2 (0.03)	0.15 (0.01)	4.9 (0.4)

cm^2). In C beams, fibres were mostly horizontally aligned; the average density was 0.43 and 0.42 fibres/cm^2 in planes α and γ, respectively, and only 0.24 fibres/cm^2 in plane β. In the T beams, the highest density was found in plane α (0.51 fibres/cm^2), and lower values in longitudinal–parallel and longitudinal–perpendicular planes (0.32 and 0.29 fibres/cm^2).

Results from FR-SCC2 also show a preferential fibre orientation in horizontal planes, but no clear influence of the casting arrangement. The fibre densities in plane α were similar for C and T beams (0.81 and 0.71 fibres/cm^2), and the fibre density at plane γ was always lower than in plane α. Finally, the mean density at planes γ and β of the V beams was 0.72, showing that in this case fibres were also oriented in horizontal planes.

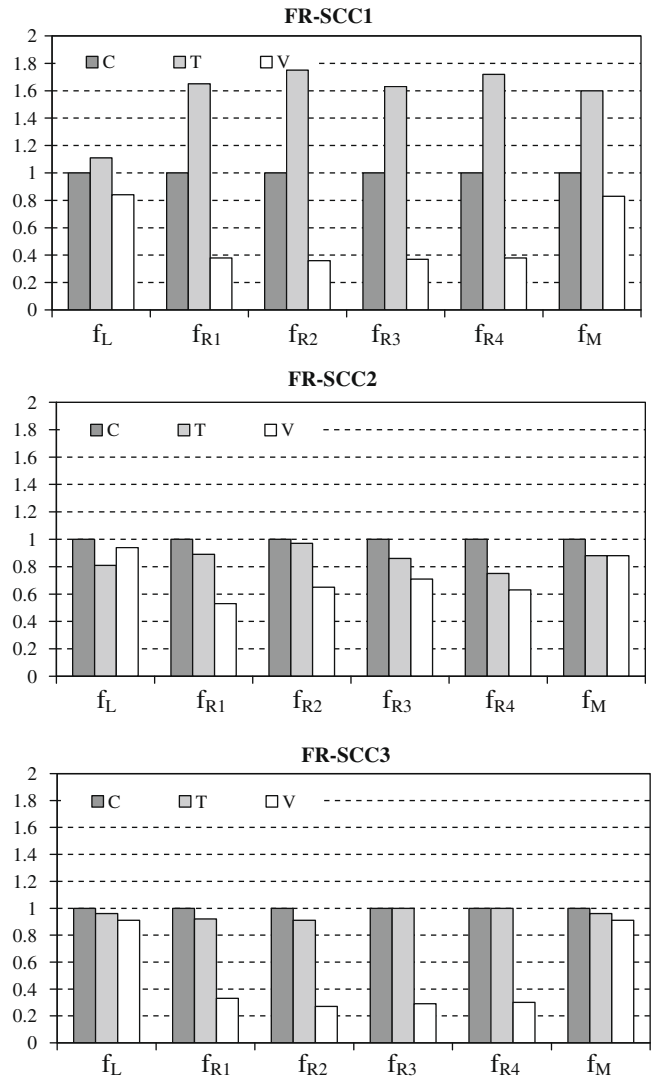

Fig. 6. Strength and toughness parameters relative to the C beams.

It must be noted that, though in a few cases the scatter of the results of fibre density was slightly high, the results undoubtedly show that the fibres orientate in preferential planes.

Fig. 7 shows the fibre density in α plane of T and V beams as relative values of the densities measured in C beams. The fibre density in FR-SCC1 of T beams was 16% higher than the density measured in C beams whereas in FR-SCC2 the fibre density in T beams was slightly lower (88%) than the density measured in C beams. In both cases the lowest values of the densities correspond to V beams, but the reduction was more evident in the case of longer fibres (47% and 70% in FR-SCC1 and FR-SCC2, respectively). As it can be observed, these values are in accordance with the relationships between the residual strengths shown in the previous section.

The fibre distribution was evaluated comparing the number of fibres counted on different zones along each plane (α, β, and γ), for the three groups of beams studied.

Fig. 8 represents the variation of the fibre density along planes β and γ (only the longitudinal variation), and along the height of plane α, for each group of beams. Mean values (big symbols) and maximum and minimum values (small symbols) corresponding to three beams of each group are plotted. Considering T and C beams of FR-SCC1, it can be seen that in T beams the highest fibre density on plane γ was found at the extreme opposite to the pouring end (end B). There seems to be a stronger wall effect on this end of the mould than at the pouring end, probably due to the concrete flow along the mould. On the other hand, the mean fibre density tends to be higher at the ends of the mould in plane γ of C beams, and less scatter was found in the density values, which can also be attributed to wall effects. Finally a low scatter of the fibre densities was observed at the bottom of the T beams, in plane α.

T beams cast with FR-SCC2 had in plane γ more fibres on every zone of the A halves (pouring end) than on the B halves. As F2 fibres are smaller with respect to the mould dimensions, there was no significant effect of the flow from one end to the other of the mould.

Regarding V beams cast with both concretes, B halves (bottom halves) showed slightly higher densities in all sections than in the case of A halves (top halves). In this case, it must be mention that a higher number of fibres was counted in the periphery of plane α of FR-SCC1, as a result of the orientation due to the wall effect.

3.3. Relationship between mesostructure and flexural test results

As it can be observed, the mechanical properties measured on the different beam groups of each concrete show that the casting arrangement and the concrete flow can affect the fibre orientation and distribution.

Fig. 9 plots individual values of the first-peak (f_L) and maximum (f_M) stresses obtained from the flexure tests, as a function of the fi-

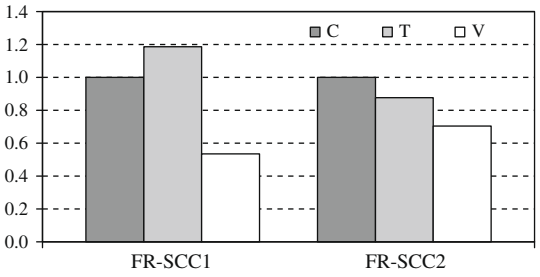

Fig. 7. Fibre density measured in plane α of beams C, T, and V cast with FR-SCC1 and FR-SCC2. Values relative to C beams.

Table 3
Fibre density measured on the different planes, fibres/cm^2 (standard deviation between parentheses).

Concrete	Beams	Plane α	Plane γ		Plane β	
			A	B	A	B
FR-SCC1	C	0.43 (0.02)	0.42 (0.10)	–	0.24 (0.04)	–
	T	0.51 (0.02)	0.32 (0.03)	0.32 (0.10)	0.28 (0.04)	0.29 (–)
	V	0.23 (0.06)	0.31 (0.12)	0.40 (0.15)	0.35 (0.01)	0.35 (0.02)
FR-SCC2	C	0.81 (0.05)	0.48 (0.06)	–	0.57 (0.08)	–
	T	0.71 (0.14)	0.50 (0.08)	0.44 (0.03)	0.47 (0.16)	0.35 (0.08)
	V	0.57 (0.09)	0.71 (–)	0.60 (0.01)	0.89 (–)	0.69 (0.04)

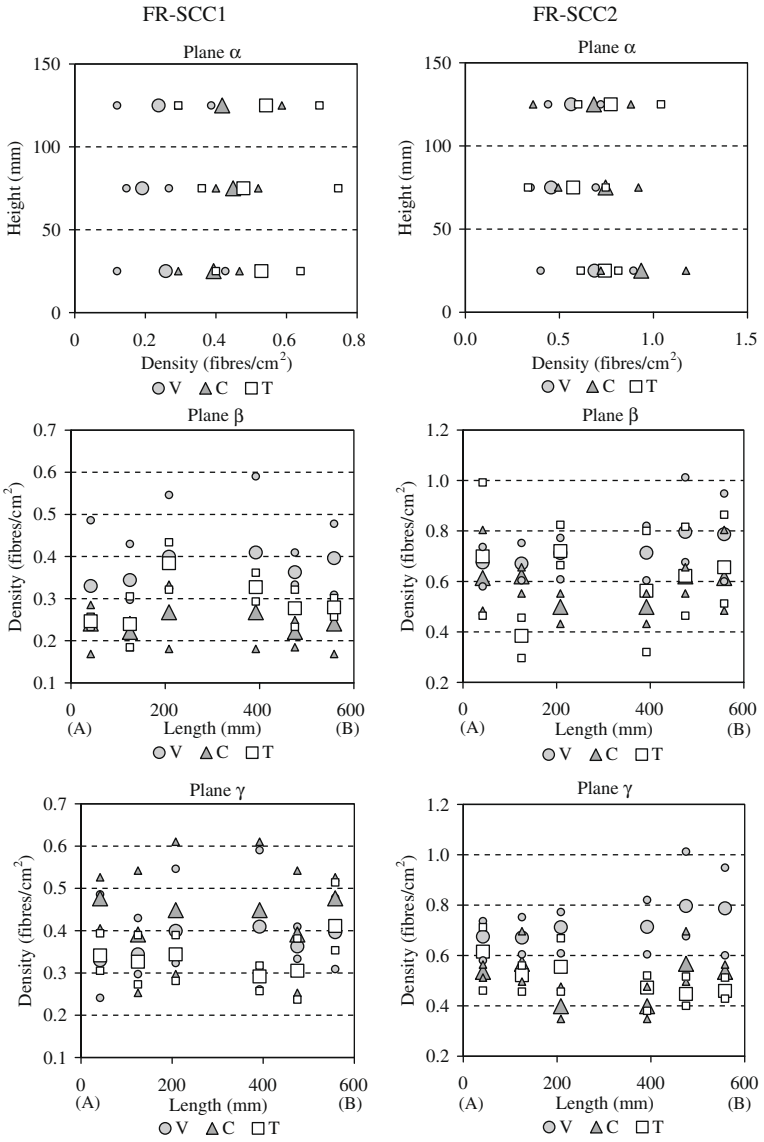

Fig. 8. Fibre distribution along α, β and γ planes for C, T and V beams cast with FR-SCC1 and FR-SCC2. Big symbols: mean fibre density, small symbols: maximum and minimum values.

bre density measured on plane α. As expected, no significant differences were observed between the first-peak flexural strengths of C, T, and V groups of each concrete, since f_L mainly depends on the plain concrete strength. The effect of the fibre density is more evident in the case of the maximum residual value, f_M, particularly for FR-SCC1.

Fig. 10 shows the relationship between the residual strength measures (f_{R1}, f_{R2}, and f_{R3}) and the fibre density for concretes FR-SCC1 and FR-SCC2. In the case of the FR-SCC1, higher residual strengths values were found in T beams, followed by C beams, which is attributed to the stronger orientation of the fibres due to the concrete flow. In V beams, the number of fibres in the transversal plane was notably lower than in the other groups, and also the residual strengths. As it was shown, the residual strengths measures of V beams were in the order of 36–38% of the residual strengths corresponding to C beams, and the fibre density in plane α was 47% lower. As the post-peak load-bearing capacity did not significantly vary with the CMOD (mainly due to the relatively large length of the FR-SCC1 steel fibre), no differences were found between the residual strengths f_{R1}, f_{R2}, and f_{R3}.

In FR-SCC2, a clear relationship between the post-peak parameters and the fibre density can also be observed. In this case, there are differences between f_{R1}, f_{R2} and f_{R3}; the post-peak behaviour of the FR-SCC2, cast with the shorter fibres, was more affected by the CMOD. The residual parameters and the fibre density were slightly higher in C beams; these facts indicate that there was almost no fibre orientation produced by the concrete flow through the pipe. Beams V showed the lowest residual capacity, with values between 53% and 71% of the residual strengths measured in C beams, and a fibre density of approximately 70% of the density measured in C beams.

As mentioned, although the fibre density was not measured in FR-SCC3 due to the practical difficulties for a precise fibre counting by visual means, a preferential orientation in horizontal planes can be inferred from the post-peak behaviour observed in flexure tests of the C, T, and V beams.

4. Conclusions

The following conclusions can be summarised from the analysis of the fibre density and post-peak mechanical response of three fi-

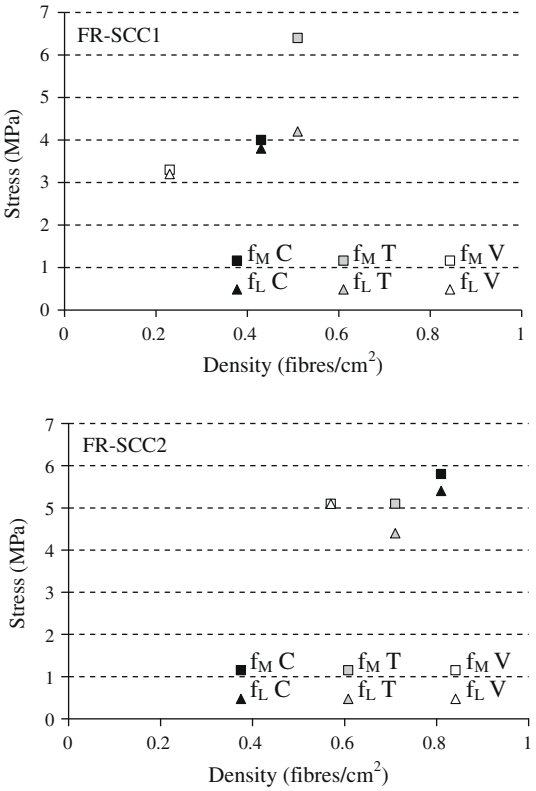

Fig. 9. First-peak and maximum residual strengths from flexure tests as a function of the fibre density.

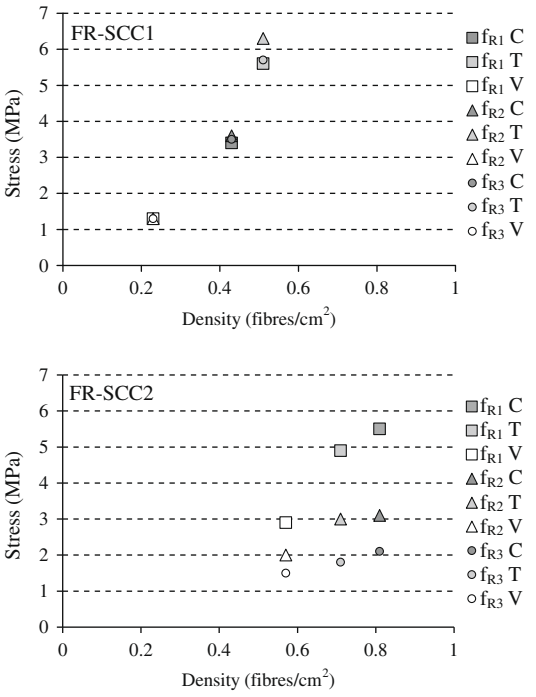

Fig. 10. Post-peak parameters from flexure tests as a function of the fibre density.

bre reinforced self-compacting concretes (FR-SCC) including different types of fibres; two steel fibres of different length, and one polymer fibre:

- As in conventional vibrated FRC, a preferential orientation (mainly in horizontal planes) was found in FR-SCC incorporating steel and polymer fibres.
- The casting procedure can significantly affect the fibre distribution and orientation. This fact can have significant implications for the mechanical performance of FR-SCC structural elements in service.
- In standard beams cast vertically (V), like a column, and tested horizontally, the fibre reinforcement was notably less efficient, from a mechanical point of view, in the three FR-SCC.
- Beams cast with FR-SCC incorporating the longer steel fibres and cast pouring the concrete through a tube (T), like a pumping pipeline, presented a higher post-peak response than beams cast from the centre of the mould (C) following the Standard procedure. However this was not observed in beams cast with shorter steel fibres or polymer fibres.
- The observed post-peak behaviours can be explained by the mesostructural characteristics of the concrete (type, distribution and orientation of fibres). Important wall effects were evidenced, that clearly depend on the ratios between the dimensions of the mould and the length of the fibres; in FR-SCC1, with 50 mm long steel fibres, significant differences were found in terms of fibre orientation between beams cast following the Standard procedure (C) and those filled from one end after the concrete had flowed through a 5 m long tube. This effect was not evident in the case of FR-SCC2, incorporating 30 mm long fibres.

The analysis of the mesostructural characteristics of FR-SCC and the comprehension of the fibre distribution/orientation sources appears as a useful tool to take more benefit out of fibre reinforcement, i.e. by defining convenient casting conditions.

Acknowledgements

Funding from the Spanish Ministry of Science and Innovation, through Grants BIA2006-15471-C02-01 and PSE 11-2005, PSE-380000-2006-4, PSE-380000-2007-1: "*HABITAT 2030*", is greatly appreciated. The authors specially thank the important contributions of Arran Cockburn and Neil Shuttleworth from the University of Sheffield, and Narasimha D.P. Tanikella, Chandni Balachandran and Shanoo P. Garg, from the Indian Institute of Technology Madras. The support of the staff of the Structural Technology Laboratory of the Technical University of Catalonia (former affiliation of the second author) is immensely acknowledged.

References

[1] Kooiman AG. Modelling steel fibre reinforced concrete for structural design. PhD thesis, department of structural and building engineering, Delft University of Technology; 2000.
[2] Dupont D, Vandewalle L. Distribution of steel fibres in rectangular sections. Cem Concr Compos 2005;27:391–8.
[3] Barr BIG, Lee MK. Round – robin analysis of the RILEM TC 162-TDF beam – bending test: Part 3 – fibre distribution. Mater Struct 2003;36:631–5.
[4] Barragán BE, Gettu R, Martín MA, Zerbino RL. Uniaxial tension test for steel fibre reinforced concrete – a parametric study. Cem Concr Compos 2003;25(7):767–77.
[5] Barragán BE. Failure and toughness of steel fiber reinforced concrete. PhD thesis, Universidad Politécnica de Cataluña; 2002.
[6] Giaccio G, Zerbino R. Caracterización de hormigones con fibras de acero basada en la recomendación RILEM TC 162-TDF empleando vigas de menor tamaño. In: Aguado A, Agulló L, Barragán B, Ramos G, editors. Tecnología de estructuras de hormigón. Barcelona; 2004. p. 235–47.
[7] Grünewald S. Performance-based design of self-compacting fibre reinforced concrete. PhD thesis, Delft University of Technology; 2004.
[8] Stähli P, van Mier JGM. Manufacturing, fibre anisotropy and fracture of hybrid fibre concrete. Eng Fract Mech 2007;74:223–42.
[9] Edgington J, Hannant DJ. Steel fibre reinforced concrete. The effect on fibre orientation of compaction by vibration. Mater Struct 1972;5(25):41–4.
[10] Gettu R, Gardner DR, Saldivar H, Barragán BE. Study of the distribution and orientation of fibers in SFRC specimens. Mater Struct 2005;38:31–7.

[11] Ozyurt N, Mason TO, Shah SP. Correlation of fiber dispersion, rheology and mechanical performance of FRCs. Cem Concr Compos 2007;29:70–9.
[12] Soroushian P, Lee C. Distribution and orientation of fibers in steel fiber reinforced concrete. ACI Mater J 1990;87(5):433–9.
[13] Prasanth TND, Gettu R. On the distribution of fibres in self compacting concrete. In: Gettu R, editor. Proceedings of 7th International RILEM symposium on fibre reinforced concrete. Chennai: India; 2008. p. 1147–53.
[14] Vandewalle L, Heirman G, Rickstal FV. Fibre orientation in self-compacting fibre reinforced concrete. In: Gettu R, editor. Proceedings of the 7th International RILEM symposium on fibre reinforced concrete. Chennai: India; 2008. p. 719–28.
[15] Yardımc MY, Baradan B, Tasdemir MA. Studies on the relation between fiber orientation and flexural performance of SFRSCC. In: Gettu R, editor. Proceedings of the 7th International RILEM symposium on fibre reinforced concrete. Chennai: India; 2008. p. 711–8.